Three Dimensional Sound Field Reproduction using Multiple Circular Loudspeaker Arrays: Functional Analysis Guided Approach

Wen Zhang, *Member, IEEE*, and Thushara D. Abhayapala, *Senior Member, IEEE*

***Abstract*—Three dimensional sound field reproduction based on higher order Ambisonics requires the placement of loudspeakers on a sphere that surrounds the target reproduction region. The deployment of a spherical array is not trivial especially for implementation in real rooms where the placement flexibility is highly desirable. This paper proposes a design of multiple circular loudspeaker arrays for reproducing three dimensional sound fields originating from a limited region of interest. We apply a functional analysis framework to formulate the sound field reproduction problem in a closed form. Secondary source distributions and target sound fields are modeled as two Hilbert spaces and mapped by an integral operator and its adjoint operator, from which a self-adjoint operator is constructed and the singular value decomposition is applied to represent source distributions and sound fields with two sets of interrelated singular functions. We derive the solutions for a circular secondary source arrangement and propose the design of placing multiple circular loudspeaker arrays only over the limited region of interest. Such a design allows for non-spherical and non-uniform loudspeaker placement and thus provides a flexible array arrangement. The reproduction accuracy of the proposed method is verified through numerical simulations.**

***Index Terms*—3D audio, ambisonics, circular loudspeaker arrays, sound field reproduction, spherical harmonics.**

I. Introduction

SPATIAL sound field reproduction aims to create an immersive sound field over a predefined spatial region so that the listener inside the region would experience a realistic but virtual replication of the original sound field. This is achieved by controlling the placement of a set of loudspeakers usually on the boundary that encloses the spatial region of interest and deriving the signals emitted from the loudspeakers. A common implementation of sound reproduction is the Ambisonic system firstly proposed by Gerzon [1], [2]. The system is based on the zero and first order spherical harmonic decomposition of the original sound field into four channels and from a linear combination of these four channels to derive the loudspeaker driving signals. This low-order system is optimum at low frequencies but produces inaccurate reproduction at high frequencies. Higher order Ambisonics (HOA) based on cylindrical two-dimensional (2D or horizontal plane) harmonic [3]–[5] or spherical three-dimensional (3D or full sphere) harmonic [6]–[9] decomposition of a sound field (normally referred as the "mode-matching" approach) was developed especially for high reproduction frequencies and large reproduction regions.

Wave-Field Synthesis (WFS) is another well-known sound reproduction technique initially conceived by Berkhout [10], [11]. The fundamental principle is based on the Kirchhoff-Helmholtz integral [12] to represent a sound field in the interior of a bounded region of the space by a continuous distribution of monopole and normally oriented dipole secondary sources, arranged on the boundary of that region [13]. An array of equally spaced loudspeakers is used to approximate the continuous distribution of secondary sources. Reproduction artifacts due to the finite size of the array and the spatial discretization of the ideally continuous distribution of secondary sources are investigated in the literature [14]. WFS technique has been mainly implemented in 2D sound reproduction using linear and planar arrays [15]–[17], for which a 2.5D operator was proposed to replace the secondary line sources by point sources (known as 2.5D WFS) [13], [18], [19]. However, very limited work has been done in implementing 3D systems due to the fact that there is a significant large number of loudspeakers required for high frequency reproduction over large regions [20]–[22].

Even though a few 3D reproduction systems were implemented based on HOA [23]–[25], there is a critical problem in terms of loudspeaker placement. To perfectly reconstruct incident sound fields, the mode-matching approach requires the placement of loudspeakers on a sphere that surrounds the target reproduction region [7], [26]. The deployment of a spherical loudspeaker array is impractical in reality. Non-spherical loudspeaker arrays have been deployed based on the least-squares approach to match pressures decomposed by the spherical harmonics over a region of space [27]. The least-squares approach seems to provide a great deal of simplicity and flexibility; however, it involves a matrix inversion and if the matrix is poorly conditioned, the solution may not exist. Tikhonov regularization is the common method for obtaining loudspeaker weights

Manuscript received February 19, 2013; revised June 20, 2013; accepted May 01, 2014. Date of publication May 14, 2014; date of current version May 23, 2014. This work was supported by the Australian Research Council's Discovery Projects funding scheme (project no. DP110103369). The associate editor coordinating the review of this manuscript and approving it for publication was Dr. Patrick A. Naylor.

The authors are with the Research School of Engineering, College of Engineering and Computer Science, The Australian National University, Canberra ACT 0200, Australia (e-mail: wen.zhang@anu.edu.au; thushara.abhayapala@anu.edu.au).

Color versions of one or more of the figures in this paper are available online at http://ieeexplore.ieee.org.

Digital Object Identifier 10.1109/TASLP.2014.2324182

with limited energy [28]. In [29], a set of numerical orthonormal band-limited modes of a partial-sphere or a hemisphere is obtained by regularizing the Gram-matrix of the spherical harmonics, from which irregular arrays are constructed. All these numerical solutions do not provide any insights into physical structure of the solution to the loudspeaker placement problem.

The functional analysis framework was firstly introduced into sound field reproduction by Fazi [22], [26], [30]. A continuous distribution of secondary sources and the produced sound field are interrelated by an integral operator, from which a self-adjoint operator is constructed and singular value decomposition can be applied to modal decompose the source distribution and sound field with two sets of orthogonal functions (called as modes or modal basis functions). The construction of source distributions allows for a perfectly accurate reproduction if the full sets of source modes and sound field modes (all modes corresponding to non-zero singular values) are included. As illustrated by the work [22], [26], the modal basis functions for source distributions and sound fields arranged on two concentric circles and spheres are cylindrical harmonics and spherical harmonics, respectively.

The goal of this work is to apply the functional analysis framework to investigate a flexible scheme of placing multiple circular loudspeaker arrays for three-dimensional sound field reproduction. This scheme was firstly proposed by Gupta and Abhayapala [31], in which spherical harmonics based mode-selection is implemented by combining driving signals from multiple loudspeaker arrays at different colatitudes to control the reproduced sound field. The approach however still involves a matrix inversion and thus depends on the condition number of the matrix to guide the placement of the loudspeakers. The aim here is by applying the functional analysis framework, we can formulate the reproduction problem in a closed form so that the matrix inversion can be avoided [32]. Besides, the solution also reveals the physical insight into array design.

The paper is organized as follows. In Section II, the theoretical fundamentals of the proposed functional analysis framework are presented. We review the concepts of modeling the secondary source distributions and target sound fields as two Hilbert spaces, a linear operator and its adjoint operator mapping between these two spaces, and applying the singular value decomposition to represent the source distributions and target sound fields. To demonstrate the application of this functional analysis based approach, we firstly present solutions for a spherical secondary source arrangement in Section III, which are consistent with standard three dimensional HOA solutions. We further derive the solutions for a circular secondary source arrangement, from which a design of multiple circular loudspeaker arrays is given in Section IV. The proposed design provides flexible geometry to suit sound field reproduction in real rooms and auditoria; in addition, by analyzing the reproduction efficiency of each circular array, the design has the ability to focus on sound fields from a limited region of interest, i.e., only loudspeakers close to the virtual source directions are active. Finally, in Section V, we present simulations to verify the derived theoretical results.

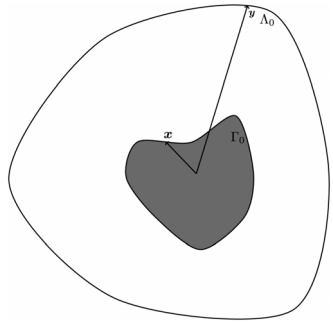

Fig. 1. Cross-section of the three-dimensional secondary source distributions and sound fields on boundaries Λ_0 and Γ_0.

II. General Theory

We start by reviewing the general functional analysis framework adopted for the sound field reproduction problem [26].

A. Secondary Source Distributions and Target Sound Fields

Consider a continuous secondary source distribution $\rho(\boldsymbol{y})$ (the complex strength of the secondary sources) on the surface Λ_0, the generated sound field $\hat{S}(\boldsymbol{x})$ can be represented as

$$\hat{S}(\boldsymbol{x}) = (\mathcal{A}\rho)(\boldsymbol{x}) = \int_{\Lambda_0} \rho(\boldsymbol{y}) G(\boldsymbol{x}|\boldsymbol{y}) d\boldsymbol{y}, \boldsymbol{y} \in \Lambda_0, \qquad (1)$$

where $\boldsymbol{x} = \{r_{\boldsymbol{x}}, \theta_{\boldsymbol{x}}, \phi_{\boldsymbol{x}}\}$ is the observation point, $\boldsymbol{y} = \{r_{\boldsymbol{y}}, \theta_{\boldsymbol{y}}, \phi_{\boldsymbol{y}}\}$ denotes a secondary source position and an integral is used to represent the summation of the infinite number of secondary sources arranged on the surface Λ_0 with $d\boldsymbol{y} = r_{\boldsymbol{y}}^2 \sin\theta_{\boldsymbol{y}} d\theta_{\boldsymbol{y}} d\phi_{\boldsymbol{y}}$. $G(\boldsymbol{x}|\boldsymbol{y})$ is a Green function that represents a spatial-temporal transfer function from $\boldsymbol{y}$ to $\boldsymbol{x}$; in free-field conditions for an omnidirectional point source it is defined as [33],

$$G(\boldsymbol{x}|\boldsymbol{y}) = \frac{e^{-ik|\boldsymbol{y}-\boldsymbol{x}|}}{4\pi|\boldsymbol{y}-\boldsymbol{x}|}, \qquad (2)$$

where $k = 2\pi f/c$ is the wavenumber with f the frequency and c the speed of wave propagation. Note that here only a single frequency f is considered and for simplicity the explicit dependence on k has been suppressed in the notation.

The Kirchhoff-Helmholtz theorem states that the sound field within a source-free volume is fully defined by the acoustic pressure and pressure gradient on the continuous surface enclosing the volume [34]. When the wavenumber is not one of the Dirichlet eigenvalues for the target region, reproducing a sound field on the surface enclosing the region of interest ensures the exact sound field reproduction within the region, i.e., $S(\boldsymbol{x}) = \hat{S}(\boldsymbol{x})$ on Γ_0[12], [26]. Hence, the control region considered here is the surface enclosing the target reproduction region, i.e. $\boldsymbol{x} \in \Gamma_0$, as shown in Fig. 1.

We apply the Hilbert space concepts to formalize source distribution functions and desired sound fields as two separate spaces [35]. A Hilbert space is a complete inner product space and many of the main results of linear algebra can be generalized to linear operations on separable Hilbert spaces. We define the space of secondary source distributions on Λ_0 by $\mathcal{D}$, denoted as $\mathcal{D} \triangleq \{\rho(\boldsymbol{y}) : \|\rho\|_{\mathcal{D}} < \infty, \boldsymbol{y} \in \Lambda_0\}$ with the associated norm defined on an inner product $\|\rho\|_{\mathcal{D}}^2 = \langle \rho, \rho \rangle_{\mathcal{D}} = \int_{\Lambda_0} \rho(\boldsymbol{y}) \overline{\rho(\boldsymbol{y})} d\boldsymbol{y}$,

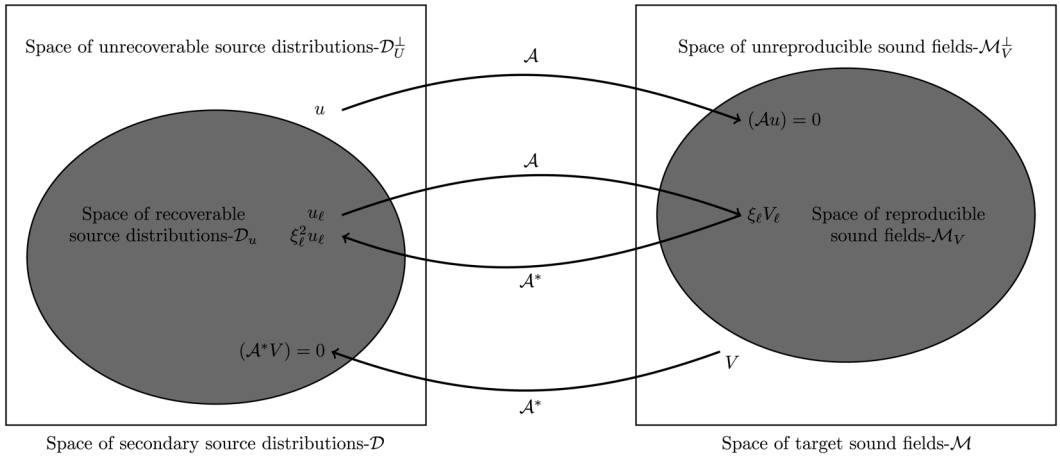

Fig. 2. The structure of the mapping between the space of secondary source distributions and the space of target sound fields.

where $\overline{(\cdot)}$ denotes the complex conjugate operation; while the space of target sound fields within the control region is represented by $\mathcal{M} \triangleq \{S(\boldsymbol{x}) : \|S\|_{\mathcal{M}} < \infty, \boldsymbol{x} \in \Gamma_0\}$, where $\|S\|_{\mathcal{M}}^2 = \langle S, S\rangle_{\mathcal{M}} = \int_{\Gamma_0} S(\boldsymbol{x})\overline{S(\boldsymbol{x})}d\boldsymbol{x}$.

B. Mapping Operator and Recovery Problem

The operator $\mathcal{A} : \mathcal{D} \rightarrow \mathcal{M}$ defines the mapping from a secondary source distribution to a target sound field as shown in Fig. 2. The sound filed reproduction in essence is a recovery problem involving the solution of an integral equation as shown in (1) (known as a Fredholm integral equation of the first kind [35]) and in most cases the problem is ill-posed. This implies that the solution may not exist, may not be unique or may not be bounded (or unstable) as disused in [26], [33]. The functional analysis framework provides a systematic way to investigate this ill-posed recovery problem as shown in the following.

Given $\mathcal{A}$ is an integral operator (or a linear transformation), applying the functional analysis framework an adjoint operator is defined to represent the inverse mapping $\mathcal{A}^* : \mathcal{M} \rightarrow \mathcal{D}$, i.e.,

$$\langle \mathcal{A}\rho, S\rangle_{\mathcal{M}} = \langle \rho, \mathcal{A}^* S\rangle_{\mathcal{D}}. \tag{3}$$

For the case under consideration, this means that the adjoint operator is given by,

$$(\mathcal{A}^* S)(\boldsymbol{y}) = \int_{\Gamma_0} S(\boldsymbol{x})G^*(\boldsymbol{y}|\boldsymbol{x})d\boldsymbol{x}, \boldsymbol{x} \in \Gamma_0 \tag{4}$$

where

$$G^*(\boldsymbol{y}|\boldsymbol{x}) = \frac{e^{ik|\boldsymbol{y}-\boldsymbol{x}|}}{4\pi|\boldsymbol{y}-\boldsymbol{x}|}. \tag{5}$$

The physical meaning of the adjoint operator $(\mathcal{A}^* S)(\boldsymbol{y}; k)$ is to treat the observation points as monopole-like sources on Γ_0 and to represent the sound field generated by these sources on the boundary of the secondary source distribution Λ_0[22].

The operator $\mathcal{A}$ is a compact operator and the same of its adjoint operator $\mathcal{A}^*$[35]. Now consider the operator $\mathcal{A}^*\mathcal{A} : \mathcal{D} \rightarrow \mathcal{D}$. Given $(\mathcal{A}^*\mathcal{A})^* = \mathcal{A}^*\mathcal{A}$ and $\mathcal{A}$ is bounded, $\mathcal{A}^*\mathcal{A}$ is a self-adjoint compact operator [35]. Thus the singular value decomposition of the operator can be applied to represent every element in both spaces with the derived modes (a set of orthonormal functions) which are interrelated and so that a closed form representation of the inverse problem can be derived.

C. Singular Value Decomposition

For the self-adjoint compact operator $\mathcal{A}^*\mathcal{A}$ on the Hilbert space $\mathcal{D}$, there exists an orthonormal system of singular functions $\{u_\ell\}$ corresponding to non-zero singular values $\{\xi_\ell\}$ such that every element $\rho \in \mathcal{D}$ has a unique representation in the form,

$$\rho(\boldsymbol{y}) = \sum_{\ell=1}^{\infty} \langle \rho, u_\ell\rangle_{\mathcal{D}} u_\ell(\boldsymbol{y}) + u(\boldsymbol{y}), \tag{6}$$

where the set of functions $u_\ell(\boldsymbol{y})$ are called the source distribution modes, and $u(\boldsymbol{y})$ satisfies the equation $(\mathcal{A}u) = 0$.

While the source distribution modes satisfy the following equation,

$$\xi_\ell^2 u_\ell = \mathcal{A}^*\mathcal{A}u_\ell; \tag{7}$$

a target sound field can also be represented by a set of sound field modes, i.e.,

$$S(\boldsymbol{x}) = \sum_{\ell=1}^{\infty} \langle S, V_\ell\rangle_{\mathcal{M}} V_\ell + V(\boldsymbol{x}), \tag{8}$$

where $\mathcal{A}^*V = 0$, or V is the orthogonal projection of S onto the null-space of $\mathcal{A}^*$.

The relationship between the source distribution modes and sound field modes can be found as

$$V_\ell = \frac{1}{\xi_\ell}\mathcal{A}u_\ell, u_\ell = \frac{1}{\xi_\ell}\mathcal{A}^* V_\ell \tag{9}$$

while

$$\langle \rho, u_\ell\rangle_{\mathcal{D}} = \frac{1}{\xi_\ell}\langle S, V_\ell\rangle_{\mathcal{M}}. \tag{10}$$

If the space of secondary source distribution is divided into two subspaces, one is the space of recoverable secondary source distributions $\mathcal{D}_u$ and the other is the space of unrecoverable secondary source distributions $\mathcal{D}_u^{\perp}$, which are orthogonal complement of $\mathcal{D}_u$. Equation (6) shows that a recoverable secondary

source distribution ρ_u is in the subspace of $\mathcal{D}_u$ spanned by the source distribution modes u_ℓ, that is

$$\rho_u(\boldsymbol{y}) = \sum_{\ell=1}^{\infty} \langle \rho, u_\ell \rangle_{\mathcal{D}} u_\ell(\boldsymbol{y}). \tag{11}$$

The corresponding reproduced sound field $S_V(\boldsymbol{x})$ satisfies the following equation,

$$S_V(\boldsymbol{x}) = (\mathcal{A}\rho_u)(\boldsymbol{y}) = \sum_{\ell=1}^{\infty} \langle S, V_\ell \rangle_{\mathcal{M}} V_\ell(\boldsymbol{x}) = S(\boldsymbol{x}) - V(\boldsymbol{x}), \tag{12}$$

and is an element of the space of reproducible sound fields $\mathcal{M}_V$ spanned by V_ℓ. Notice that here we consider the target sound fields due to a virtual source outside the reproduction region; the space of target sound fields $\mathcal{M}$ can be partitioned into the space of reproducible sound fields $\mathcal{M}_V$ and space of unreproducible sound fields $\mathcal{M}_V^{\perp}$, i.e., $\mathcal{M} = \mathcal{M}_V + \mathcal{M}_V^{\perp}$[1]. The developed concepts and the structure of the mapping between the space of secondary source distributions and the space of target sound fields are illustrated in Fig. 2.

This implies that for a target field $S(\boldsymbol{x})$ on Γ_0 that can be completely represented as a linear combination of the sound field modes $V_\ell(\boldsymbol{x})$ (i.e., $V(\boldsymbol{x}) = 0$ or $S \in \mathcal{M}_V$), a corresponding source distribution $\rho_u(\boldsymbol{y})$ can be identified based on (10) and (11)

$$\rho_u(\boldsymbol{y}) = \sum_{\ell=1}^{\infty} \frac{1}{\xi_\ell} \langle S, V_\ell \rangle_{\mathcal{M}} u_\ell(\boldsymbol{y}) \tag{13}$$

such that the reproduced sound field $S_V(\boldsymbol{x}) = S(\boldsymbol{x})$ on Γ_0. This means that the solution always exists if the target sound field is in the range of $\mathcal{A}$. In addition, the target sound field decomposed coefficients $\langle S, V_\ell \rangle_{\mathcal{M}}$ need to exhibit a steeper decay than the decay of the singular value ξ_ℓ so that the inverse problem has a bounded or stable solution [26].

III. Three Dimensional Sound Field Reproduction

Analytical derivation of source distribution modes and sound field modes is possible only for simple geometries, such as spherical or circular boundaries. In this work, we assume that the control region is the surface of a sphere enclosing the target reproduction region, i.e. $\Gamma_0 \equiv \Omega_r$, where $\Omega_r = \{r\boldsymbol{x} = r, \hat{\boldsymbol{x}} \in \mathbb{S}^2\}$ is the sphere of radius r and $\mathbb{S}^2$ represents the unit sphere. Next, we apply the functional analysis framework introduced in Sec. II to spherical and circular secondary source distributions.

A. Spherical Secondary Source Arrangement

We firstly review the case of secondary sources arranged on a sphere [26]. The free field Green function (2) can be expanded as [12]

$$\frac{e^{-ik|\boldsymbol{y}-\boldsymbol{x}|}}{4\pi|\boldsymbol{y}-\boldsymbol{x}|} = \sum_{n=0}^{\infty} \sum_{m=-n}^{n} -ikh_n^{(2)}(kr\boldsymbol{y}) j_n(kr) \overline{Y_n^m(\hat{\boldsymbol{y}})} Y_n^m(\hat{\boldsymbol{x}}), \tag{14}$$

where $j_n(\cdot)$ and $h_n^{(2)}(\cdot)$ are the first kind spherical Bessel function and second kind spherical Hankel function of the nth degree, respectively. The unit vectors are denoted by $\hat{\boldsymbol{x}}$ and $\hat{\boldsymbol{y}}$.

The spherical harmonics are defined as [12]

$$Y_n^m(\hat{\boldsymbol{x}}) = \mathcal{P}_{nm}(\cos\theta_{\boldsymbol{x}}) E_m(\phi_{\boldsymbol{x}}), \tag{15}$$

where

$$\mathcal{P}_{nm}(\cos\theta_{\boldsymbol{x}}) = \sqrt{\frac{2n+1}{2} \frac{(n-|m|)!}{(n+|m|)!}} P_n^{|m|}(\cos\theta_{\boldsymbol{x}}), \tag{16}$$

is the normalized associated Legendre function and $E_m(\phi_{\boldsymbol{x}}) = e^{im\phi_{\boldsymbol{x}}}/\sqrt{2\pi}$ is the normalized complex exponential function.

For a spherical secondary source arrangement, i.e., $\Lambda_0^{\mathrm{sd}} \equiv \Omega_{R_s}$, where $\Omega_{R_s} = \{r_{\boldsymbol{y}} = R_s, \hat{\boldsymbol{y}} \in \mathbb{S}^2\}$ represents a sphere of radius R_s and $R_s > r$, we have the equations in (17) for the source distribution modes and sound field modes[2]. Here, $\int_{\mathbb{S}^2} d\hat{\boldsymbol{y}} = \int_0^{2\pi} \int_0^{\pi} \sin\theta_{\boldsymbol{y}} d\theta_{\boldsymbol{y}} d\phi_{\boldsymbol{y}}$.

Based on the orthogonality of the spherical harmonics,

$$\int_{\mathbb{S}^2} Y_n^m(\hat{\boldsymbol{y}}) \overline{Y_{n'}^{m'}(\hat{\boldsymbol{y}})} d\hat{\boldsymbol{y}} = \delta_{nn'} \delta_{mm'}, \tag{18}$$

we can analytically derive the singular values and modes as

$$\begin{aligned} \xi_\ell^{\mathrm{sd}} &= k j_n(kr) |h_n^{(2)}(kR_s)| \\ u_\ell^{\mathrm{sd}}(\hat{\boldsymbol{y}}) &= Y_n^m(\hat{\boldsymbol{y}}) \\ V_\ell^{\mathrm{sd}}(\hat{\boldsymbol{x}}) &= \frac{-ih_n^{(2)}(kR_s)}{|h_n^{(2)}(kR_s)|} Y_n^m(\hat{\boldsymbol{x}}). \end{aligned} \tag{19}$$

with $\ell = n^2 + n + m + 1$, $n = 0, \ldots, \infty$ and $m = -n, \ldots, n$.

[1]The target sound field due to a virtual source located inside the reproduction region has zero projection onto $M_V^{\perp}$ but is still not reproducible as no bounded source density exists to generate it [26].

[2]Note that the constants R_S^2 and r^2 in the surface spherical integration are removed so that we could have the same formulation as in the HOA system [8].

$$\begin{aligned} (\mathcal{A}u_\ell^{\mathrm{sd}})(\boldsymbol{x}) &= \sum_{n=0}^{\infty} \sum_{m=-n}^{n} -ikh_n^{(2)}(kR_s) j_n(kr) Y_n^m(\hat{\boldsymbol{x}}) \int_0^{2\pi} \int_0^{\pi} u_\ell^{\mathrm{sd}}(\boldsymbol{y}) \overline{Y_n^m(\hat{\boldsymbol{y}})} \sin\theta_{\boldsymbol{y}} d\theta_{\boldsymbol{y}} d\phi_{\boldsymbol{y}}. \\ (\mathcal{A}^* V_\ell^{\mathrm{sd}})(\boldsymbol{y}) &= \sum_{n=0}^{\infty} \sum_{m=-n}^{n} ikh_n^{(1)}(kR_s) j_n(kr) Y_n^m(\hat{\boldsymbol{y}}) \int_0^{2\pi} \int_0^{\pi} V_\ell^{\mathrm{sd}}(\boldsymbol{x}) \overline{Y_n^m(\hat{\boldsymbol{x}})} \sin\theta_{\boldsymbol{x}} d\theta_{\boldsymbol{x}} d\phi_{\boldsymbol{y}}. \\ (\mathcal{A}^* \mathcal{A} u_\ell^{\mathrm{sd}})(\boldsymbol{y}) &= \sum_{n=0}^{\infty} \sum_{m=-n}^{n} k^2 |h_n^{(2)}(kR_s) j_n(kr)|^2 Y_n^m(\hat{\boldsymbol{y}}) \int_0^{2\pi} \int_0^{\pi} u_\ell^{\mathrm{sd}}(\boldsymbol{y}) \overline{Y_n^m(\hat{\boldsymbol{y}})} \sin\theta_{\boldsymbol{y}} d\theta_{\boldsymbol{y}} d\phi_{\boldsymbol{y}}. \end{aligned} \tag{17}$$

The spaces $\mathcal{D}$ and $\mathcal{M}$ have infinite number of dimensions in the strict sense. Here, we adopt a rule of thumb given in [36] [3] to represent a sound field within the reproduction region using the spherical harmonic expansion up to the degree $N = \lceil ekr/2 \rceil$. That is, functions in $\mathcal{D}$ and $\mathcal{M}$ can be approximately represented by the first $L = (N+1)^2$ modes for this sound field reproduction problem.

By substituting (19) into (13), we can derive the secondary source distribution for reproducing a target sound field $S(\boldsymbol{x})$,

$$\begin{aligned}\rho_u^{\mathrm{sd}}(\boldsymbol{y}) &= \sum_{\ell=1}^{L} \frac{1}{\xi_\ell^{\mathrm{sd}}} \langle S, V_\ell^{\mathrm{sd}} \rangle_{\mathcal{M}_V} u_\ell^{\mathrm{sd}}(\hat{\boldsymbol{y}}) \\ &= \sum_{n=0}^{N} \sum_{m=-n}^{n} \frac{\beta_{nm} Y_n^m(\hat{\boldsymbol{y}})}{-ikh_n^{(2)}(kR_s) j_n(kr)}, \end{aligned} \tag{20}$$

where

$$\beta_{nm} = \int_0^{2\pi} \int_0^{\pi} S(\hat{\boldsymbol{x}}) \overline{Y_n^m(\hat{\boldsymbol{x}})} \sin\theta_{\boldsymbol{x}} d\theta_{\boldsymbol{x}} d\phi_{\boldsymbol{x}} \tag{21}$$

are spherical wave spectrum of the desired sound field at $r_{\boldsymbol{x}} = r$, i.e., its spherical harmonic expansion coefficients.

This result is the standard 3D HOA solution based on spherical harmonic decomposition of a sound field. The solution for the spherical secondary source distribution always exists and is bounded when the virtual source is located in the exterior of Λ_0[26]. A special case is at the positions of Bessel zeros, i.e., $j_n(kr)$ are zero where $kr \neq 0$, the solutions are not unique. This corresponds to the case that the secondary source distribution has a non-trivial projection on the null-space of $\mathcal{A}_s$, or the produced sound field is not observable on the control region Ω_{R_s}. Different strategies could be used to overcome the nonuniqueness as illustrated in [37]. Because the source distribution function constructed from (20) is a continuous spatial function, a main research problem is about the sampling of this aperture function for placing discrete loudspeaker sources equidistantly on a sphere known as a spherical loudspeaker array [7].

B. Circular Secondary Source Arrangement

For a circular secondary source arrangement, i.e., $\Lambda_0^{\mathrm{cd}} = \{r_{\boldsymbol{y}} = R_c, \theta_{\boldsymbol{y}} = \theta, \phi_{\boldsymbol{y}} \in [0, 2\pi)\}$ with radius $R_c > r$, we have the following equations written in (22). Here, $\int_{\Lambda_0^{\mathrm{cd}}} d\hat{\boldsymbol{y}} = \int_0^{2\pi} d\phi_{\boldsymbol{y}}$.

Based on the orthogonality of the complex exponential functions,

$$\int_0^{2\pi} E_m(\phi) \overline{E'_m(\phi)} d\phi = \delta_{mm'}, \tag{23}$$

we can analytically derive the modes and singular values as

$$\begin{aligned} \xi_\ell^{\mathrm{cd}} &= \sqrt{\sum_{n=|\ell|}^{\infty} k^2 \left| h_n^{(2)}(kR_c) j_n(kr) \mathcal{P}_{n\ell}(\cos\theta) \right|^2} \\ u_\ell^{\mathrm{cd}}(\hat{\boldsymbol{y}}) &= E_\ell(\phi_{\boldsymbol{y}}) \\ V_\ell^{\mathrm{cd}}(\hat{\boldsymbol{x}}) &= \frac{\sum_{n=|\ell|}^{\infty} -ih_n^{(2)}(kR_c) j_n(kr) \mathcal{P}_{n\ell}(\cos\theta) Y_n^\ell(\hat{\boldsymbol{x}})}{\sqrt{\sum_{n=|\ell|}^{\infty} \left| h_n^{(2)}(kR_c) j_n(kr) \mathcal{P}_{n\ell}(\cos\theta) \right|^2}} \end{aligned} \tag{24}$$

Based on the fact that a spatial sound field within the reproduction region can be approximated using its spherical harmonics expansion coefficients up to the degree $N = \lceil ekr/2 \rceil$[36], the circular secondary source distribution is approximately represented by the first $L = 2N+1$ modes, i.e., $\ell = -N, \ldots, N$. It is now possible to calculate analytically the secondary source distribution as

$$\rho_u^{\mathrm{cd}}(\boldsymbol{y}) = \sum_{\ell=-N}^{N} \gamma_\ell E_\ell(\phi_{\boldsymbol{y}}), \tag{25}$$

where the coefficients can be determined directly from the desired sound field decomposed with the derived modes or inferred from the spherical wave spectrum of the desired sound field

$$\begin{aligned} \gamma_\ell &= \frac{1}{\xi_\ell^{\mathrm{cd}}} \langle S, V_\ell^{\mathrm{cd}} \rangle_{\mathcal{M}_V} \\ &= \frac{\sum_{n=|\ell|}^{N} i h_n^{(1)}(kR_c) j_n(kr) \mathcal{P}_{n\ell}(\cos\theta) \beta_{n\ell}}{\sum_{n=|\ell|}^{N} k \left| h_n^{(2)}(kR_c) j_n(kr) \mathcal{P}_{n\ell}(\cos\theta) \right|^2}. \end{aligned} \tag{26}$$

The detailed derivation is given in Appendix. A.

Given the sound field reproduction in most cases is the ill-conditioned recovery problem, we have the following remarks for the circular secondary source arrangement.

- The range of the operator $\mathcal{A}_c$ is quite different from $\mathcal{A}_s$, i.e., the case of a circular or a spherical source distribution, which results in that the space of reproducible sound fields

[3] The truncation theorem in [36] states that for representation of a wave field generated by far field sources the relative truncation error is no more than 16.1% once N equals the critical threshold $\lceil ekr/2 \rceil$, and thereafter decreases at least exponentially to zero as N increases.

$$\begin{aligned} (\mathcal{A} u_\ell^{\mathrm{cd}})(\boldsymbol{x}) &= \sum_{n=0}^{\infty} \sum_{m=-n}^{n} -ikh_n^{(2)}(kR_c) j_n(kr) \mathcal{P}_{nm}(\cos\theta) Y_n^m(\hat{\boldsymbol{x}}) \int_0^{2\pi} u_\ell^{\mathrm{cd}}(\boldsymbol{y}) \overline{E_m(\phi_{\boldsymbol{y}})} d\phi_{\boldsymbol{y}}. \\ (\mathcal{A}^* V_\ell^{\mathrm{cd}})(\boldsymbol{y}) &= \sum_{n=0}^{\infty} \sum_{m=-n}^{n} ikh_n^{(1)}(kR_c) j_n(kr) Y_n^m(\hat{\boldsymbol{y}}) \int_0^{2\pi} \int_0^{\pi} V_\ell^{\mathrm{cd}}(\boldsymbol{x}) \overline{Y_n^m(\hat{\boldsymbol{x}})} \sin\theta_{\boldsymbol{x}} d\theta_{\boldsymbol{x}} d\phi_{\boldsymbol{y}}. \\ (\mathcal{A}^* \mathcal{A} u_\ell^{\mathrm{cd}})(\boldsymbol{y}) &= \sum_{n=0}^{\infty} \sum_{m=-n}^{n} k^2 \left| h_n^{(2)}(kR_c) j_n(kr) \mathcal{P}_{n|m|}(\cos\theta) \right|^2 E_m(\phi_{\boldsymbol{y}}) \int_0^{2\pi} u_\ell^{\mathrm{cd}}(\boldsymbol{y}) \overline{E_m(\phi_{\boldsymbol{y}})} d\phi_{\boldsymbol{y}}. \end{aligned} \tag{22}$$

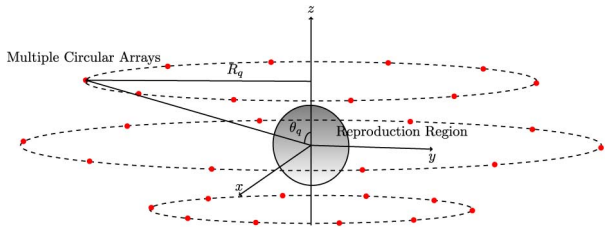

Fig. 3. Scheme of multiple circular loudspeaker arrays for sound field reproduction over the surface of a sphere.

are very different in the two cases. This can be understood as the radiation pattern of a circular source arrangement and a spherical source distribution are different and only virtual sources within the effective radiation pattern can be reproduced with high accuracy.

- From (24), it can be seen that the singular values are not zero even if $j_n(kr) = 0$ for some n. This seems to imply that the uniqueness issue related to the Dirichlet eigenvalues is not an issue in the case of circular secondary source arrangement, as opposed to the case of spherical secondary source distribution.

IV. Multiple Circular Array Configuration

For synthesis of three-dimensional sound fields, a design of multiple circular array configuration is proposed in the following.

A. Array Placement and Selective Activation

Multiple circular loudspeaker arrays are placed over the entire range of virtual source colatitudes, i.e., $\theta_q,\ q = 1, 2, \ldots, Q$. The interval between two arrays is

$$\Delta\theta < \frac{2}{N}. \tag{27}$$

As explained in Appendix. B, this condition guarantees that a sound field due to a virtual source at a colatitude between two circular arrays are within the effective radiation pattern of both arrays and thus can be jointly reconstructed from these two arrays. In terms of the array geometry, as shown in Fig. 3, besides subject to the maximum interval between two adjacent arrays, the arrays can have different radii as long as the requirement $R_q > r$ is satisfied. This configuration would provide significantly improved flexibility for loudspeaker placement in real acoustic environments.

Instead of using panning functions, the loudspeaker array activation is based on a parameter called the reproduction efficiency, i.e., the L_2 norm of the sound field decomposed coefficients,

$$\eta_q = \sqrt{\sum_{\ell=-N}^{N} |\mu_\ell^{(q)}|^2} = \sqrt{\sum_{\ell=-N}^{N} |\langle S, V_\ell^{(q)} \rangle_{\mathcal{M}}|^2}. \tag{28}$$

Notation $(\cdot)^{(q)}$ is added to denote the corresponding modes and singular values for the loudspeaker array at θ_q. Given the fact that the set of sound field modes $V_\ell^{(q)}$ are an orthonormal system for each individual array, the reproduction efficiency describes how much energy of a sound field is projected in the space of reproducible sound fields when using each array and can be used for comparison of different arrays.

We calculate the efficiency ratio, i.e. $\eta_q / \max(\eta_1, \ldots, \eta_Q)$, and our simulation suggests that a criteria for loudspeaker array activation is the efficacy ratio larger than 90%. This corresponds to the case that a loudspeaker array is activated only when the virtual source is from a direction which is within the main beam of the array radiation pattern. In the meantime, this selective activation method makes the proposed design suitable to both modal-based reproduction and data-based reproduction as explained in Sec. IV-C.

B. Loudspeaker Weight Design

For activated loudspeaker arrays, the corresponding secondary source distribution can be determined by

$$\rho_u^{(q)}(\boldsymbol{y}) = \frac{1}{N_q} \sum_{\ell=-N}^{N} \gamma_\ell^{(q)} E_\ell(\phi_{\boldsymbol{y}}), \tag{29}$$

with

$$\gamma_\ell^{(q)} = \frac{\langle S, V_\ell^{(q)} \rangle_{\mathcal{M}}}{\xi_\ell^{(q)}}, \tag{30}$$

where the amplitudes of the source distribution are scaled by dividing by the number of activated arrays N_q.

In practical implementation, the continuous secondary source distributions are discretized to determine the loudspeaker driving signals. Note that $\rho_u^{(q)}(\boldsymbol{y})$ in each circular array is a periodic function of $\phi_{\boldsymbol{y}}$ with period of 2π. Given that the continuous source distributions are mode limited to N, only $2N + 1$ coefficients $\gamma_\ell^{(q)}$ can sufficiently describe the source distribution. According to the Shannon sampling theorem [38], we need to place $P \geq 2N + 1$ loudspeakers equiangularly on the circle so that we can exactly reproduce $\rho_u^{(q)}(\boldsymbol{y})$; this leads to the design of the pth loudspeaker weights in the qth array as

$$w_p^{(q)}(k) = \rho_u^{(q)}(\boldsymbol{y}_p)\Delta\phi, p = 1, \ldots, P, \tag{31}$$

where $\Delta\phi = 2\pi/P$ is the angular spacing of loudspeakers and $\boldsymbol{y}_p = \{R_q, \theta_q, \phi_p\}$ with $\phi_p = (p-1)\Delta\phi$. Note that we can apply (31) to non-uniform loudspeaker placement in the array as long as the maximum separation angle is no more than $\Delta\phi$.

C. Implementation Remarks

Secondary source distributions and the corresponding loudspeaker driving signals are uniquely determined by the spherical wave spectrum of the desired sound field. We have the following remarks.

1) Modal-based Reproduction: In modal-based reproduction, wave fields from virtual sources are described analytically. The spherical wave spectrum of the desired sound field can be written in the following form [33]

$$\beta_{n\ell}(k) = \begin{cases} 4\pi i^n j_n(kr)\overline{Y_n^\ell(\theta_{\mathrm{pw}}, \phi_{\mathrm{pw}})}, & \text{plane wave} \\ -ikj_n(kr)h_n^{(2)}(kr_s)\overline{Y_n^\ell(\theta_{\mathrm{sw}}, \phi_{\mathrm{sw}})}, & \text{spherical wave.} \end{cases} \tag{32}$$

In terms of reconstructing a sound field produced by multiple virtual sources, the above approach is only required to perform once based on the knowledge of the total sound field and its spherical wave spectrum.

2) Data-based Reproduction

The proposed approach is not restricted to virtual sound sources; it can also be applied to reproduce sound fields captured by microphone arrays. Given the geometry of the reproduction region and the purpose here is to calculate the spherical wave spectrum, an arrangement of a spherical microphone array is the most preferable choice [39].

3) Number of Loudspeakers: Reproduction of virtual sources over a full range of colatitudes requires approximately $\mathcal{O}(\pi(N+1)^2)$ loudspeakers. This is almost three times of the least number of loudspeakers required in a spherical array. However, the proposed implementation provides a flexible arrangement for virtual sources originating from a limited range of colatitudes, for example $[\theta_l, \theta_h]$, for which a reduced number of loudspeakers are required, i.e., $\mathcal{O}((\theta_h - \theta_l)(N+1)^2)$.

The procedure of implementation is summarized in Algorithm 1. Note that the method developed for a single frequency signal can be repeated and applied in parallel over a subband decomposition for wide-band sources.

Algorithm 1 Implementation Procedures

Step 1 Choose the focused region of interest $[\theta_l, \theta_h]$, the frequency of operation f and radius of the reproduction region r.

Step 2 Determine the expansion order N and loudspeaker array placement within $[\theta_l, \theta_h]$ subject to the condition (27).

Step 3 Obtain the spherical wave spectrum of the desired sound field.

Step 4 Calculate the reproduction efficiency of each individual array η_q.

$N_q = 0$;

$\boldsymbol{\eta} = [\eta_1, \ldots, \eta_Q]$;

for $q = 1$:Q

if $\eta_q / \max(\boldsymbol{\eta}) \geq 0.9$

Active the q the array and calculate source distribution coefficients (30);

$N_q = N_q + 1$;

else The qth array remains inactive; **end**

end

Step 5 Determine secondary source distributions (29) and loudspeaker weights (31).

V. Simulation Results

A. Simulation Setup

To evaluate the performance of the proposed scheme, an example of multiple circular arrays of loudspeakers is examined in a simple simulation setup. Free-field source conditions are assumed; the desired sound field is a spherical waver or plane wave resulting from a virtual monopole source over the 3D reproduction region. The frequency of operation is set to $f = 500$ Hz and the reproduction region is limited to a sphere of radius $r = 0.5$ m. This gives $kr = 4.58$, and the rule of thumb suggests using $N = \lceil ekr/2 \rceil = 7$, thus requiring the maximum interval between two adjacent arrays is less than $2/N$ (or $16.37°$). In the simulation, we limit the virtual source colatitude within the range of $[60°, 90°]$ and thus place three arrays at an interval of $15°$ within that range; different radii are assigned to these arrays, i.e., $R_1 = 2$ m for $\theta_1 = 60°$, $R_2 = 3$ m for $\theta_2 = 75°$, and $R_3 = 2$ m for $\theta_3 = 90°$. 15 loudspeakers are equiangularly placed in these circular arrays.

We investigate two kinds of situations, I) the virtual source is at a colatitude where a loudspeaker array is located, for example $(\theta_v, \phi_v) = (75°, 90°)$ and II) the virtual source is located between two adjacent arrays, for example, $(\theta_v, \phi_v) = (85°, 135°)$. The relative mean square error (MSE) of the reproduction over the desired reproduction region is used as the error metric,

$$\varepsilon(kr) \triangleq \frac{\int_0^r \int_0^{2\pi} \int_0^{\pi} |S_r(\boldsymbol{x}) - S_d(\boldsymbol{x})|^2 d\boldsymbol{x}}{\int_0^r \int_0^{2\pi} \int_0^{\pi} |S_d(\boldsymbol{x})|^2 d\boldsymbol{x}}, \tag{33}$$

where the integration is over a spherical ball of radius r and $d\boldsymbol{x} = r_{\boldsymbol{x}}^2 \sin\theta_{\boldsymbol{x}} d\theta_{\boldsymbol{x}} d\phi_{\boldsymbol{x}} dr_{\boldsymbol{x}}$. $S_d(\boldsymbol{x})$ and $S_r(\boldsymbol{x})$ are the desired and reproduced sound fields, respectively.

B. Example Sound Field

We firstly reconstruct a spherical wave of frequency 500 Hz within the spherical reproduction region of radius $r = 0.5$ m. The virtual source of unit strength is located at $r_v = 3.1$ m and $(\theta_{sw}, \phi_{sw}) = (75°, 60°)$ or $(\theta_{sw}, \phi_{sw}) = (85°, 135°)$. The real parts of the reproduced sound fields in the $x-y$ plane are shown in Fig. 4. These figures are displayed as density plots, where the display is limited to the maximum value of the reconstructed field within the reproduction region, i.e., acoustic pressure greater than 0.02 are white and less than -0.02 are black. The normalized mean-square reproduction error of the two examples are given in Fig. 5(a) and (b), respectively. Within the reproduction region, the synthesized sound fields and the desired sound fields are very close with the average relative MSE around 10^{-3} and 0.01 in these two examples, respectively.

The next example is to demonstrate the designed loudspeaker array performance for reproducing a plane wave of unit strength from the direction $(\theta_{pw}, \phi_{pw}) = (75°, 90°)$ and $(\theta_{pw}, \phi_{pw}) = (85°, 135°)$. As demonstrated in Figs. 6 and 7, within the reproduction region the synthesized sound fields agree reasonably well with the desired sound fields, for example the average relative MSE are 0.01 and 0.04 for those two cases. As expected, the error in reproducing plane wave fields is generally larger than that in reproducing spherical wave fields. This is due to the fact that the basis functions developed in this work are based on the spherical wave propagation model (the kernel of the operator $\mathcal{A}$). The desired plane wave field have components which cannot be fully reproduced by the near-field secondary source distributions in the current setup. However, with the average error less than 0.04, still quite accurate reproduction is achieved using the proposed method.

Simulation results demonstrate that the reproduction efficiency based selection method only activates loudspeakers in close proximity to the virtual source. For example, when the

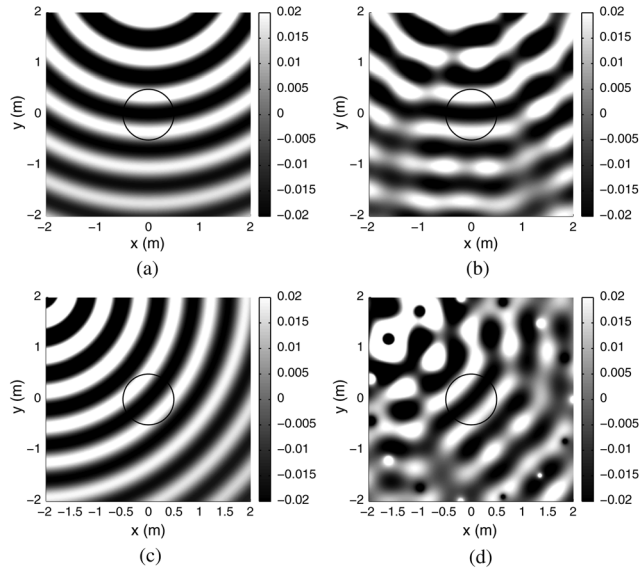

Fig. 4. Reproduction of a spherical wave of frequency 500 Hz. (a) and (c) are desired sound fields corresponding to a virtual source located at $r_{\rm v} = 3.1$ m and $(\theta_{\rm sw}, \phi_{\rm sw}) = (75^\circ, 90^\circ)$ and $(\theta_{\rm sw}, \phi_{\rm sw}) = (85^\circ, 135^\circ)$, respectively. (b) and (d) are reproduced sound fields corresponding to (a) and (c). The encircled region is the reproduction region.

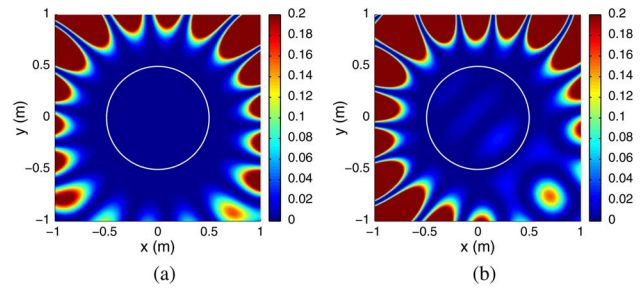

Fig. 5. Normalized mean-square reproduction error for synthesis of a spherical wave at 500 Hz. (a) A spherical wave arriving from $r_{\rm v} = 3.1$ m and the direction $(\theta_{\rm sw}, \phi_{\rm sw}) = (75^\circ, 90^\circ)$. (b) A spherical wave arriving from $r_{\rm v} = 3.1$ m and the direction $(\theta_{\rm sw}, \phi_{\rm sw}) = (85^\circ, 135^\circ)$. The encircled region is the reproduction region.

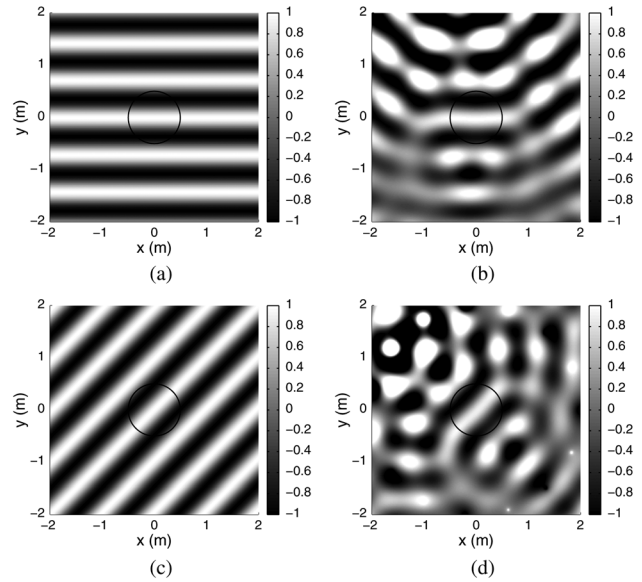

Fig. 6. Reproduction of a plane wave of frequency 500 Hz. (a) and (c) are desired sound fields corresponding to a plane wave from $(\theta_{\rm pw}, \phi_{\rm pw}) = (75^\circ, 90^\circ)$ and $(\theta_{\rm pw}, \phi_{\rm pw}) = (85^\circ, 135^\circ)$, respectively. (b) and (d) are reproduced sound fields corresponding to (a) and (c). The encircled region is the reproduction region.

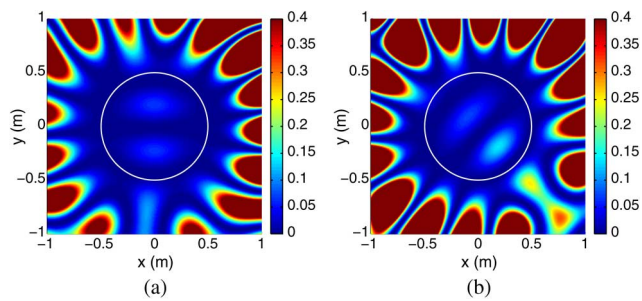

Fig. 7. Normalized mean-square reproduction error for synthesis of a plane wave at 500 Hz. (a) A plane wave arriving from the direction $(\theta_{\rm pw}, \phi_{\rm pw}) = (75^\circ, 90^\circ)$. (b) A plane wave arriving the direction $(\theta_{\rm pw}, \phi_{\rm pw}) = (85^\circ, 135^\circ)$. The encircled region is the reproduction region.

virtual source is located at the same colatitude as a loudspeaker array (example 1), only that array ($\theta_2 = 75^\circ$) is activated; while for the case that the virtual source is from a colatitude between two arrays but not very close to either of them (example 2), both arrays ($\theta_2 = 75^\circ$ and $\theta_3 = 90^\circ$) are activated.

C. Comparison with the Least-Squares Solutions

We specifically compare the proposed method with the least-squares solutions [7] to the sound reproduction problem using the same loudspeaker array positions as in the previous examples. The goal of the least-squares approach is to match every angular mode of a sound field (i.e., the decomposed spherical harmonic coefficients) generated by the loudspeaker array to the corresponding mode of the desired sound field in the least-squares sense, from which the loudspeaker weights are determined. Fig. 8 plots the reproduction of the previous examples using the least-squares approach. Comparing with results in Figs. 4–7, it can be seen that both the proposed method and least-squares method have comparable performance. The least-squares method is especially better for reproducing plane wave fields. However, the least-squares technique activates all three layers of loudspeakers and has the largest levels of sound outside the reproduction zone. Regularization on a bounded loudspeaker weight energy can reduce the loudspeaker weights to generate small levels of sound field outside the reproduction zone but at the expense of reproduction error [28]. The proposed method on the other hand actives only loudspeakers in close proximity to the virtual source. These results demonstrate that the functional analysis guided approach provides an insight into physical structure of the solution to the loudspeaker placement. In addition, the proposed method has lower computation complexity as the matrix inversion is avoided which makes it a good candidate for synthesis of real time 3D moving sound.

D. Reproduction Error

We next investigate the performance of the proposed scheme for reproducing sound fields at various frequencies and radii. Figure 9 plots the reproduction error versus kr for synthesis of a spherical wave and a plane wave under two situations as mentioned in Sec. V-A. We note that the system designed at a particular frequency and radius ($kr = 4.58$ in the example) can provide accurate sound field reproduction for numbers less than

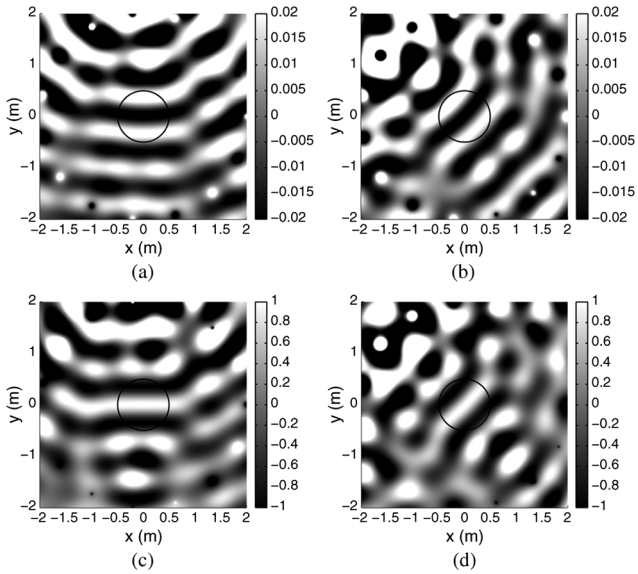

Fig. 8. Least-squares based sound field reproduction. (a) and (b) Reproduction of a spherical wave corresponding to Fig. 4. (c) and (d) Reproduction of a plane wave corresponding to Fig. 6. The encircled region is the reproduction region.

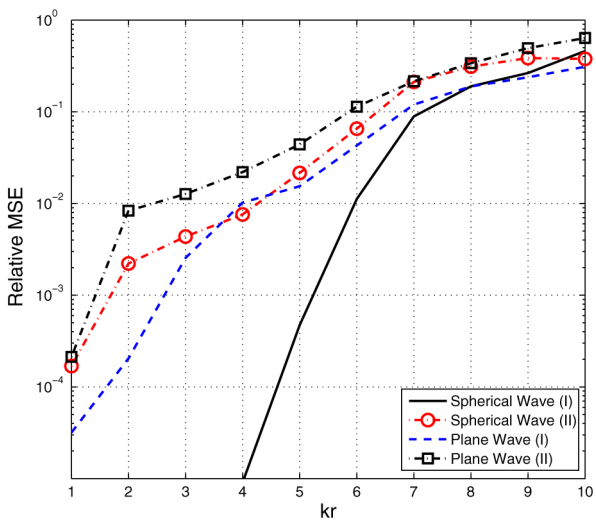

Fig. 9. Reproduction error of the system designed at 500 Hz and 0.5 m reproduction region as a function of kr.

the designed value. At the large kr beyond the designed value, the synthesized wavefronts are highly distorted and the reproduction error becomes significant. The general trend is that the error monotonically increases with kr. This again validates the rule of thumb proposed in the paper for choosing the required truncation order of expansion in (25).

VI. Conclusion

A practically realizable design of multiple circular loudspeaker arrays is proposed for reproducing 3D sound fields. The design is based on a functional analysis framework to solve the sound field reproduction problem for a circular secondary source arrangement. The recoverable secondary source distributions and reproducible sound fields are modal decomposed by the derived interrelated source distribution modes and sound field modes, from which the sound field reproduction problem is formulated. The proposed design of multiple circular arrays provides a flexible array geometry with the ability to focus on the sound field incident from a limited region of interest. In addition, based on the parameter, the reproduction efficiency, this design activates only the loudspeakers in close proximity to the virtual source. We show design examples of spherical wave and plane wave reproduction at an operating frequency of 500 Hz with the reproduction region limited to 0.5 m using the proposed multiple circular array scheme.

Appendix

A. Proof of Equation (26)

The coefficients of the secondary source distribution is obtained from

$$\gamma_\ell = \frac{1}{\xi_\ell^{\mathrm{cd}}} \langle S, V_\ell^{\mathrm{cd}} \rangle_{\mathcal{M}}, \tag{34}$$

where by substituting (24) and applying the truncation of infinite summation to the degree N, the modal decomposition of the desired sound field can be written as

$$\begin{aligned}\langle S, V_\ell^{\mathrm{cd}} \rangle_{\mathcal{M}} &= \int_{\mathbb{S}^2} S(\hat{\boldsymbol{x}}) \overline{V_\ell^{\mathrm{cd}}(\hat{\boldsymbol{x}})} d\hat{\boldsymbol{x}} \\ &= \frac{\sum_{n=|\ell|}^{N} i h_n^{(1)}(kR_c) j_n(kr) \mathcal{P}_{n\ell}(\cos\theta) \int_{\mathbb{S}^2} S(\hat{\boldsymbol{x}}) \overline{Y_n^\ell(\hat{\boldsymbol{x}})} d\hat{\boldsymbol{x}}}{\sqrt{\sum_{n=|\ell|}^{N} \left| h_n^{(2)}(kR_c) j_n(kr) \mathcal{P}_{n\ell}(\cos\theta) \right|^2}} \\ &= \frac{\sum_{n=|\ell|}^{N} i h_n^{(1)}(kR_c) j_n(kr) \mathcal{P}_{n\ell}(\cos\theta) \beta_{n\ell}}{\sqrt{\sum_{n=|\ell|}^{N} \left| h_n^{(2)}(kR_c) j_n(kr) \mathcal{P}_{n\ell}(\cos\theta) \right|^2}}.\end{aligned} \tag{35}$$

Therefore, we have

$$\gamma_\ell = \frac{\sum_{n=|\ell|}^{N} i h_n^{(1)}(kR_c) j_n(kr) \mathcal{P}_{n\ell}(\cos\theta) \beta_{n\ell}}{\sum_{n=|\ell|}^{N} k \left| h_n^{(2)}(kR_c) j_n(kr) \mathcal{P}_{n\ell}(\cos\theta) \right|^2}. \tag{36}$$

B. Proof of Equation (27)

For a circular secondary source distribution at a colatitude θ and represented by (25), its radiation pattern can be written as

$$(\mathcal{A}_c \rho_u^{\mathrm{cd}})(\boldsymbol{x}) = \sum_{\ell=-N}^{N} \sum_{n=|\ell|}^{N} -ik\gamma_\ell h_n^{(2)}(kR_c) j_n(kr) \mathcal{P}_{n\ell}(\cos\theta) Y_n^\ell(\hat{\boldsymbol{x}}). \tag{37}$$

If we assume an infinite number of circular arrays to construct a continuous aperture in θ, the problem is about the sampling of this aperture function. Notice that the radiation pattern in the colatitude direction is represented by the associated Legendre function of degree n and order ℓ. The associated Legendre function of the highest degree and order, i.e., $\mathcal{P}_{NN}(\cos\theta)$, has the narrowest main beam [12], which defines the effective radiation pattern of a circular array. In the mode-matching approach, every angular mode of the desired sound field needs to be matched. Using two circular arrays to reproduce a virtual source between them means that the modes generated by these two arrays and that of the desired sound field in the colatitude

direction have to be within the same beam (especially the main beam) so that the desired sound field can be reproduced with high accuracy.

We define the function [40]

$$g_N(\theta) = \mathcal{P}_{NN}(\cos\theta) = \frac{(-1)^N(2N)!}{2^N(N)!}(\sin\theta)^N. \qquad (38)$$

and derive the beam width of $g_N(\theta)$ from its first zero, which is used as the guideline of the maximum angular interval between two circular arrays.

The Taylor series expansion of $(\sin\theta)^N$ around $\pi/2$ gives

$$(\sin\theta)^N \approx 1 - \frac{N}{2}(\frac{\pi}{2} - \theta)^2, \qquad (39)$$

from which we can find that the zeros of $g_N(\theta)$ around $\pi/2$ are approximately at $\pm 2/N$. The derivation shows that an appropriate design is to place multiple circular arrays over the desired range of colatitudes with an interval of $\Delta\theta < 2/N$ so that a virtual source at a colatitude between any two circular arrays can be jointly reproduced from these two arrays.

ACKNOWLEDGMENT

The authors would like to thank the anonymous reviewers for their valuable comments and suggestions that helped to improve the clarity and quality of this manuscript.

REFERENCES

[1] M. A. Gerzon, "Periphony: With-height sound reproduction," *J. Audio Eng. Soc.*, vol. 21, no. 1, pp. 2–10, 1973.

[2] M. A. Gerzon, "Ambisonics in multichannel broadcastingand video," *J. Audio Eng. Soc.*, vol. 33, no. 11, pp. 859–871, 1985.

[3] D. B. Ward and T. D. Abhayapala, "Reproduction of a plane-wave sound field using an array of loudspeakers," *IEEE Trans. Speech Audio Process.*, vol. 9, no. 6, pp. 697–707, Sep. 2001.

[4] T. Betlehem and T. D. Abhayapala, "Theory and design of sound field reproduction in reverberant rooms," *J. Acoust. Soc. Amer.*, vol. 117, no. 4, pp. 2100–2111, 2005.

[5] Y. Wu and T. D. Abhayapala, "Theory and design of soundfield reproducion using continuous loudspeakers concept," *IEEE Trans. Audio, Speech, Lang. Process.*, vol. 17, no. 1, pp. 107–116, Jan. 2009.

[6] J. Daniel, "Spatial sound encoding including near field effect: Introducing distance coding filters and a viable, new ambisonic format," in *Proc. 23rd Int. Conf.: Signal Process. Audio Record. Reproduct.*, Copenhagen, Denmark, May 2003, paper No. 16.

[7] M. A. Poletti, "Three-dimensional surround sound systems based on spherical harmonics," *J. Audio Eng. Soc.*, vol. 53, no. 11, pp. 1004–1025, 2005.

[8] J. Ahrens and S. Spors, "An analytical approach to sound field reproduction using circular and spherical loudspeaker distributions," *Acta Acust. united with Acust.*, vol. 94, pp. 988–999, 2008.

[9] J. Ahrens and S. Spors, "Applying the ambisonics approach to planar and linear distributions of secondary sources and combinations thereof," *Acta Acust. united with Acust.*, vol. 98, pp. 28–36, 2012.

[10] A. J. Berkhout, "A holographic approach to acoustic control," *J. Audio Eng. Soc.*, vol. 36, no. 12, pp. 977–995, 1988.

[11] A. J. Berkhout, D. de Vries, and P. Vogel, "Acoustic control by wave field synthesis," *J. Acoust. Soc. Amer.*, vol. 93, no. 5, pp. 2764–2778, 1993.

[12] E. G. Williams, *Fourier Acoustics: Sound Radiation and Nearfield Acoustical Holography*. San Diego, CA, USA: Academic, 1999.

[13] S. Spors, R. Rabenstein, and J. Ahrens, "The theory of wave field synthesis revisited," in *Proc. 124th Conv. Audio Eng. Soc.*, Amsterdam, Netherlands, May 2008, paper No. 7358.

[14] S. Spors and R. Rabenstein, "Spatial aliasing aritifacts produced by linear and circular loudspeaker arrays used for wave field synthesis," in *Proc. 120th Conv. Audio Eng. Soc.*, Paris, France, May 2006, paper No. 6711.

[15] M. M. Boone, E. N. G. Verheijen, and P. F. V. Tol, "Spatial sound-field reproduction by wave-field synthesis," *J. Audio Eng. Soc.*, vol. 43, no. 12, pp. 1003–1012, 1995.

[16] D. de Vries and M. M. Boone, "Wave field sytnehsis and analysis using array technology," in *Proc. IEEE Workshop Applicat. Signal Process. Audio Acoust. (WASPAA)*, New Paltz, NY, USA, Oct. 1999, pp. 15–18.

[17] M. M. Boone, "Multi-actuator panels (MAPs) as loudspeaker arrays for wave field synthesis," *J. Audio Eng. Soc.*, vol. 52, no. 7–8, pp. 712–723, 2004.

[18] E. W. Start, "Direct sound enhancement by wave field synthesis," Ph.D. dissertation, Delft Univ. of Technol., Delft, The Netherlands, 1997.

[19] S. Spors and J. Ahrens, "Analysis and improvement of pre-equalization in 2.5-dimensional wave field synthesis," in *Proc. 128th Conv. Audio Eng. Soc.*, London, U.K., 2010, paper No. 8121.

[20] N. Epain and E. Friot, "Active control of sound inside a sphere via control of the acoustic pressure at the boundary surface," *J. Sound Vibr.*, vol. 299, no. 3, pp. 587–604, 2007.

[21] M. Naoe, T. Kimura, Y. Yamakata, and M. Katsumoto, "Performance evaluation of 3D sound field reproduction system using a few loudspeakers and wave field synthesis," in *Proc. 2nd Int. Symp. Universal Commun.*, Osaka, Japan, Dec. 2008, pp. 36–41.

[22] F. M. Fazi, P. A. Nelson, J. E. N. Christensen, and J. Seo, "Surround system based on three-dimensional sound field reconstruction," in *Proc. 125th Conv. Audio Eng. Soc.*, San Francisco, CA, USA, Oct. 2008, paper No. 7555.

[23] D. Excell, "Reproduction of a 3D sound field using an array of loudspeakers," Honours thesis, Australian National Univ., Canberra , Australia, 2003.

[24] Z. Li, R. Duraiswami, and N. Gumerov, "Capture and recreation of higher order 3D sound fields via reciprocity," in *Proc. Int. Conf. Audio Display*, Sydney, Australia, Jul. 2004, pp. 6–9.

[25] X. Amatriain, J. Kuchera-Morin, T. Höllerer, and S. T. Pope, "The AlloSphere: Immersve multimedia for scientific discovery and artistic exploration," *IEEE Multimedia*, vol. 16, no. 2, pp. 64–75, Apr./Jun. 2009.

[26] F. M. Fazi, "Sound field reproduction," Ph.D. dissertation, Univ. of Southampton, Southampton , U.K., 2010.

[27] J. Hannemann and K. D. Donohue, "Virtual sound source rendering using a multiple-expansion and method-of-moments approach," *J. Audio Eng. Soc.*, vol. 56, no. 6, pp. 473–481, 2008.

[28] T. Betlehem and C. Withers, "Sound field reproduction with energy constraint on loudspeaker weights," *IEEE Trans. Audio, Speech, Lang. Process.*, vol. 20, no. 8, pp. 2388–2392, Oct. 2012.

[29] H. Pomberger, F. Zotter, and A. Sontacchi, "An ambisonics format for flexible playback layouts," in *Proc. 1st Ambisonics Symp.* , Graz, Austria, Jun. 2009.

[30] F. M. Fazi and P. A. Nelson, "Application of functional analysis to the sound field reconstruction," in *Proc. 23rd Conf. Reproduced Sound: Hall of Sound - Audio for Live Events, Inst. Acoust.*, Gateshead, U.K., Nov. 2007.

[31] A. Gupta and T. D. Abhayapala, "Three-dimensional sound field reproduction using multiple circular loudspeaker arrays," *IEEE Trans. Audio, Speech, Lang. Process.*, vol. 19, no. 5, pp. 1149–1159, Jul. 2011.

[32] W. Zhang, T. Abhayapala, and F. Fazi, "Functional analysis guided approach for sound field reproduction with flexible loudspeaker layouts," in *Proc. IEEE Workshop Applicat. Signal Process. Audio Acoust. (WASPAA)*, New Paltz, NY, USA, Oct. 2013, pp. 1–4.

[33] D. Colton and R. Kress, *Inverse acoustic and electromagnetic scattering theory*, 2nd Ed. ed. Berlin, Germany: Springer-Verlag, 1998.

[34] P. A. Nelson and S. J. Elliot, *Active Control of Sound*. San Diego, CA: Academic, 1992.

[35] L. Debnath and P. Mikusiński, *Introduction to Hilbert Spaces with Applications*, 3rd Ed. ed. San Diego, CA, USA: Academic, 2005.

[36] R. A. Kennedy, P. Sadeghi, T. D. Abhayapala, and H. M. Jones, "Intrinsic limits of dimensionality and richness in random multipath fields," *IEEE Trans. Signal Process.*, vol. 55, no. 6, pp. 2542–2556, Aug. 2007.

[37] F. M. Fazi and P. A. Nelson, "Nonuniqueness of the solution of the sound field reproduction problem with boundary pressure control," *Acta Acoust. United with Acoust.*, vol. 98, pp. 1–14, 2012.

[38] C. E. Shannon, "Communication in the presence of noise," *Proc. IEEE*, vol. 86, no. 8, pp. 447–457, Aug. 1949.

[39] B. Rafaely, "Analysis and design of spherical microphone arrays," *IEEE Trans. Speech Audio Process.*, vol. 13, no. 1, pp. 135–143, 2005.

[40] I. S. Gradshteyn, I. M. Ryzhik, A. Jeffrey, and D. Zwillinger, *Table of Integrals, Series, and Products*, 6th Ed. ed. San Diego, CA, USA: Academic, 2000.

Wen Zhang (S'06–M'09) received the B.E. degree in telecommunication engineering from Xidian University, Xian, China, in 2003 and the M.E. degree in electrical engineering (with first class honors) and the Ph.D. degree from the Australian National University, Canberra, in 2005 and 2010, respectively. From 2010 to 2012, she was an OCE Postdoctoral Fellow at CSIRO Process Science and Engineering, Sydney, Australia. She is currently a research fellow in the Research School of Engineering at the Australian National University. Her primary research interests are in the fields of spatial sound-field recording and reconstruction, source separation and localization, and active noise cancellation. She is an editorial board member for *Science Journal of Circuits*, *Systems and Signal Processing* and *Advances in Signal Processing*, Horizon Research Publishing (2013-2016).

Thushara D. Abhayapala (M'00–SM'08) received the B.E. degree (with Honors) in Engineering in 1994 and the Ph.D. degree in Telecommunications Engineering in 1999, both from the Australian National University (ANU), Canberra. He is a Professor and the Director of the Research School of Engineering at ANU. He was the Leader of the Wireless Signal Processing (WSP) Program at the National ICT Australia (NICTA) from November 2005 to June 2007. His research interests are in the areas of spatial audio and acoustic signal processing, space-time signal processing for wireless communication systems, and array signal processing. He has supervised over 30 research students and coauthored over 200 peer reviewed papers. Professor Abhayapala is an Associate Editor of the IEEE/ACM TRANSACTIONS ON AUDIO, SPEECH, AND LANGUAGE PROCESSING and the *EURASIP Journal on Wireless Communications and Networking*. He is also a Member of the Audio and Acoustic Signal Processing Technical Committee (2011-2015) of the IEEE Signal Processing Society. He is a Fellow of the Engineers Australia.